Lysosomal Targeting and Trafficking of Acid Sphingomyelinase to Lipid Raft Platforms in Coronary Endothelial Cells

Si Jin, Fan Yi, Fan Zhang, Justin L. Poklis and Pin-Lan Li

The online version of this article, along with updated information and services, is located on the World Wide Web at:

http://atvb.ahajournals.org/cgi/content/full/28/11/2056

Data Supplement (unedited) at:

http://atvb.ahajournals.org/cgi/content/full/ATVBAHA.108.172478/DC1

Lysosomal Targeting and Trafficking of Acid Sphingomyelinase to Lipid Raft Platforms in Coronary Endothelial Cells

Si Jin, Fan Yi, Fan Zhang, Justin L. Poklis, Pin-Lan Li

Objective—The purpose of this study was to determine whether lysosome trafficking and targeting of acid sphingomyelinase (ASMase) to this organelle contribute to the formation of lipid raft (LR) signaling platforms in the membrane of coronary arterial endothelial cells (CAECs).

Methods and Results—By measurement of fluorescent resonance energy transfer (FRET), it was found that in FasL-stimulated CAECs, membrane lamp1 (a lysosome marker protein) or Fas and GM1 (a LR marker) were trafficking together. Cofocal colocalization assay showed that ceramide was enriched in these LR platforms. Further studies demonstrated that these ceramide molecules in LR platforms were colocalized with ASMase, a ceramide producing enzyme. Fluorescence imaging of living CAECs loaded with lysosomal specific dyes demonstrated that lysosomes fused with membrane on FasL stimulation. In the presence of lysosome function inhibitors, bafilomycin (Baf) or glycyl-L-phenylalanine-β-naphthylamide (GPN), these FasL-induced changes were abolished. Moreover, this FasL-induced formation of LR platforms was also blocked in ECs transfected with siRNA of sortilin, an intracellular transporter for targeting of ASMase to lysosomes. Functionally, FasL-induced impairment of vasodilator response was reversed by lysosomal inhibitors or sortilin gene silencing.

Conclusions—Lysosomal trafficking and targeting of ASMase are importantly involved in LRs clustering in ECs membrane, leading to the formation of signaling platforms or signalosomes. (*Arterioscler Thromb Vasc Biol*. 2008;28:2056-2062)

Key Words: Fas ligand ■ lysosome ■ coronary circulation ■ vascular endothelium ■ sphingolipid

Lipid rafts (LRs) consist of dynamic assemblies of cholesterol, lipids with saturated acyl chains, such as sphingolipids and glycosphingolipids, in the exoplasmic leaflet of the membrane bilayer, and cholesterol in the inner leaflet.[1] It has been demonstrated that the most important role of LRs in plasma membrane of cells is their function in signal transduction.[2–7] These membrane LRs can be clustered to form relatively large macrodomains on activation of individual receptors by ligand binding. These macrodomains recruit or aggregate various signaling molecules to form signaling platforms for transmembrane signal transduction.[1–3] These signaling platforms have been reported for different signaling pathways in a variety of cell types such as ion channels activation in cardiac cells,[8,9] apoptotic signaling in T-cells,[10–12] death receptor activation in endothelial cells,[2] neurotransmitter signaling in neurons,[4] insulin signaling in beta cells,[13–16] and several carcinogenic signaling in tumor cells.[17–21]

Recent studies in our laboratory have indicated that LRs clustering in response to activation of death receptor activation mediates the formation of signaling platforms in coronary arterial endothelial cells (CAECs). One of such signaling platforms in these cells was named as LR redox signaling platforms,[22,23] which were commented as a possible missing link between death receptor domains and NAD(P)H oxidase in endothelial cells.[24] It was demonstrated that the formation of LR signaling platforms is associated with ceramide production by hydrolysis of sphingomyelin via acid sphingomyelinase (ASMase).[25,26] The production of ceramide in the cell membrane forms ceramide-enriched microdomains, which are able to spontaneously fuse to large macrodomains, namely, clusters or platforms.[1] It is known that ASMase gene gives rise to one common precursor protein, namely SMase precursor-mannose. This gene product can be shuttled into either a lysosomal trafficking pathway mediated by sortilin[27] or a secretory pathway.[28] By using lysosome function inhibitors, we demonstrated that lysosomal vesicles have an important impact on the formation of these ceramide-enriched signaling platforms in CAECs.[29] However, it remains unknown how lysosomal vesicles participate in the formation of these LR platforms and whether lysosomes could fuse into LRs and release ASMase to mediate the

production of ceramide. It is also unclear where lysosomal ASMase is derived from and how these ASMases are trafficking through lysosomes to LR to form ceramide, ultimately leading to the formation of ceramide-enriched raft signaling platforms. The present study was designed to address these questions.

Materials and Methods

Cell Culture
The primary cultures of bovine CAECs were obtained as we described previously.[22,23,25,29] All studies were performed by using CAECs of 2 to 4 passages.

Fluorescence Resonance Energy Transfer Analysis
CAECs were stained with TRITC-labeled CTXB and fluorescein isothiocyanate (FITC)-labeled antilamp1 (a lysosomal marker protein), anti-CD95 (Fas) antibodies as we described previously and then visualized by confocal microscope.[22,23,29] To accurately observe the staining on the cell membrane, these cells were not permeabilized by excluding detergent in the washing and incubation buffer (PBS). Basically, the fusion of lysosomes or secretory vesicles into the plasma membrane results in exposure of lysosomal proteins onto the outer leaflet of the cell membrane when cells were stimulated. It is a general phenomenon that lysosomal proteins can be detected on the outer leaflet of the cell membrane when lysosome-membrane fusion happens. An acceptor bleaching protocol was used to measure the fluorescence resonance energy transfer (FRET) efficiency as described previously.[30–33] The FRET efficiency was calculated through the following formula: $E = (FITCpost - FITCpre)/FITCpost \times 100\%$, as described previously.[31]

Confocal Analysis of LR Clusters and Its Colocalization With Ceramide or ASMase in CAECs
Detection of LR clusters were performed as we described previously.[22,25,29] Doses of compounds used in these experiments were based on our previous studies[29] and some preliminary data showing that they could effectively inhibit corresponding cell responses. Colocalization was analyzed by Image Pro Plus software.

RNA Interference of Sortilin
The siRNAs of sortilin gene were purchased from INVITROEN (CAT#HSS109429), which were confirmed to be effective in silencing sortilin gene in different cells by the company. The scrambled small RNA was confirmed as nonsilencing double-stranded RNA and used as control in the present study. Transfection of siRNA was performed using the QIAGEN TransMessenger transfection kit according to the manufacturer's instructions.

RNA Isolation and Real-Time RT-PCR Analysis
The mRNA levels for Sortilin were analyzed by real-time quantitative RT-PCR. The mRNA levels were presented as Tn as calculated by using 18S mRNA as the reference system as we presented previously.[2,34]

Western Blot Analysis
The procedures for Western Blot analysis were described in details in our previous publications.[22,23,25]

Quenching and Dequenching of FM1-43 in BCAECs
As described previously,[35,36] BCAECs were loaded with 8 μmol/L FM1-43 in 1640 medium with 10% FBS for more than 2 hours at 37°C. After washed with FBS free medium, a low laser power (λ excitation=488 nm) was used to avoid possible fluorescent bleaching. For quenching experiments, after cells were loaded with 8 μmol/L FM1-43 for 2 hours, 1 mmol/L BPB was added in the
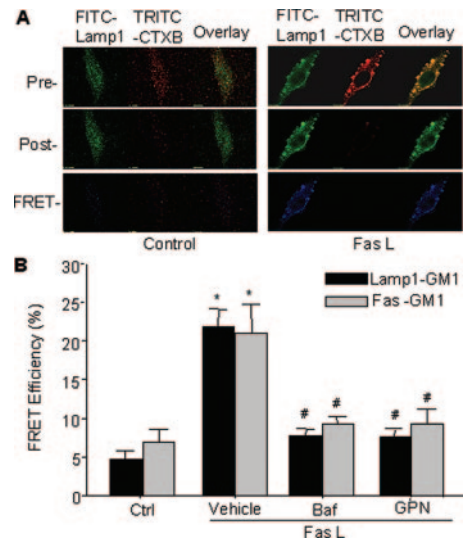

Figure 1. A, Representative images of FRET analysis between FITC-lamp1 and TRITC-CTXB in CAECs. The left group of images obtained from control CAECs and the right group of images from FasL-stimulated (10 ng/mL for 15 minutes) cells. B, Summarized results of detected FRET efficiency between CTXB and lamp1, Fas in CAECs with or without treatment of lysosome function inhibitors. Baf indictes bafilomycin; GPN, glycyl-L-phenylalanine-β-naphthylamide. n=6 batches of cells, *$P<0.05$ vs control; #$P<0.05$ vs vehicle+FasL group.

extracellular medium. For dequenching experiments, cells were loaded simultaneously with 8 μmol/L FM1-43 and 1 mmol/L BPB for 2 hours.

Coronary Arterial Preparation and Microperfusion
Fresh bovine hearts were obtained from a local abattoir. Coronary arteries were prepared for microperfusion to evaluate the endothelium-dependent vasodilator response as we described previously.[22,23,29] For some vessels, a novel ultrasound microbubble technology was used to transfect the intact endothelium with scrambled small RNA or sortilin-siRNA as we and others described previously.[37–40]

Statistics
Data are presented as means±SE. Significant differences between and within multiple groups were examined using ANOVA for repeated measures, followed by Duncan multiple-range test. A Student t test was used to detect significant differences between 2 groups. $P<0.05$ was considered statistically significant.

Results

FasL-Induced FRET Between Lamp1 and LR Component
As shown in Figure 1A, FRET was detected by confocal microscopy between a fluorophore pair, FITC as donor and TRITC as acceptor, which shares the character to allow fluorescence resonance energy transfer. Acceptor (TRITC) bleaching protocol was applied to calculate the FRET efficiency. The left group of images shows a control cell costained with FITC-lamp1 and TRITC-CTXB that underwent an acceptor bleaching protocol. Both the pre- and postbleaching images were presented on the top and middle panels. FRET image (in blue) was generated by subtraction of fluorescent intensity in the prebleaching image from that in

the postbleaching image of FITC-lamp1 labeling. The overlaid images show the colocalization of both lamp1 and CTXB detected under different protocols. As shown in FRET image (blue in the bottom image), there was very low FRET detected under control condition. The right group of images shows a FasL-stimulated cell that underwent the same FRET protocol. In addition to detected patch formation of green fluorescence and colocalization of both molecules seen in the overlaid images (top panel) in response to FasL, a more intense FRET image (blue one the bottom) was detected in this FasL-treated CAEC, demonstrating that energy transfer occurs between a lysosomal marker-lamp1, and LR component-GM1 ganglioside. This close relationship between lysosome and membrane components may be due to a fusion of lysosome to the cell membrane under this condition.

FRET Between LR Molecules

As summarized in Figure 1B, the FRET efficiency between GM1 and lamp1 or Fas were significantly increased on FasL stimulation (n=6). Three pairs of molecules including GM1 versus lamp1 or Fas exhibited similar FRET efficiency with a maximum of 23.8% compared to control (5.2%). In the presence of lysosome inhibitors, Baf or GPN, FasL-induced increase in FRET efficiency was significantly attenuated for all three pairs of molecules.

Lysosome-Derived Ceramide Production in LR Platforms

As shown in Figure 2A, CAECs were stained by an Al488-labeled CTXB (as lipid raft marker) and an anticeramide antibody with Cy3 II° antibody. Under control conditions, both Al488 and Cy3 stainings were diffuse and their colocalization in overlaid images was in tiny yellow spots. When the cells were stimulated by FasL, a number of large patches or spots with colocalization of both components (yellow in overlaid image) on the cell membrane were detected. However, when these CAECs were pretreated with lysosome function inhibitors, Baf or GPN, for 20 minutes, fluorescent patch formation in response to FasL was abolished as shown in the lower panels of images.

Association of Ceramide With Local ASMase

As shown in Figure 2B, CAECs stained with Cy3-conjugated ceramide and FITC-labeled ASMase were stimulated with FasL in the presence or absence of lysosome inhibitors, Baf or GPN. The overlay of the 2 images resulted in yellow areas, which indicated clustering or colocalization of ceramide with local ASMase. It was shown that FasL increased colocalization of ASMase and ceramide, which was blocked by both lysosome function inhibitors, Baf and GPN.

Sortilin siRNA Blocked FasL-Induced Ceramide Production in LR Platforms

As shown in supplemental Figure IIA through IIC (available online at http://atvb.ahajournals.org), by real-time PCR and Western blot analysis, the silencing effect of sortilin siRNA was verified. Both the mRNA and protein level can be knocked down by more than 80%. Figure 3A presents the results obtained from experiments with sortilin gene silenc-
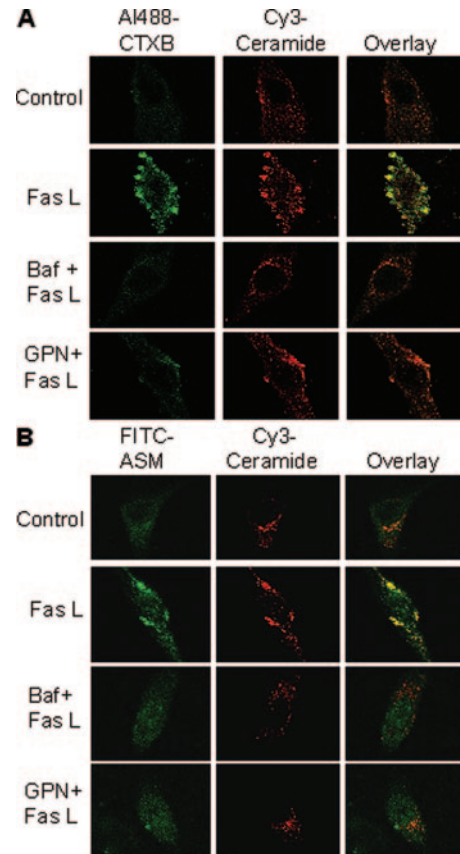

Figure 2. A, Representative confocal microscopic images of LR clusters in CAECs. Alexa488-CTX was shown as a pseudo green color on the left; Cy3-conjugated anticeramide shown as red color in the middle; and overlaid images shown on the right. Yellow spots or patches in overlaid images were defined as LRs clusters. B, ASMase and ceramide colocalization detected by confocal microscopy in CAECs. FITC-anti-ASMase was shown as green fluorescence on the left; Cy3-conjugated anticeramide red in the middle; and overlaid images on the right. Yellow spots or patches in overlaid images indicated colocalization of ASMase and ceramide in LRs.

ing, depicting the confocal microscopic analysis of Cy3-conjugated ceramide and Al488-CTXB labeled LR clusters in CAECs stimulated with FasL. Similar to Figure 3, under control condition both CTXB and ceramide stainings were diffuse. When these cells were stimulated by FasL, LR patches were detected with colocalization of ceramide. After these CAECs were transfected with sortilin siRNA, FasL-induced formation of LR platforms with ceramide colocalized was almost completely blocked. However, in scrambled sRNA transfected cells, FasL-induced formation of LR platforms remained unchanged.

Sortilin siRNA Blocked FasL-Induced FRET in LR Platforms

As summarized in Figure 3B, FasL significantly increased the FRET efficiency between GM1-gangliosides and lamp1 or CD95, in CAECs without transfection of sortilin siRNA (vehicle and scrambled sRNA-treated cells). In sortilin siRNA transfected CAECs, however, FasL-induced increase in FRET efficiency was significantly decreased to a level close to that obtained in control cells.
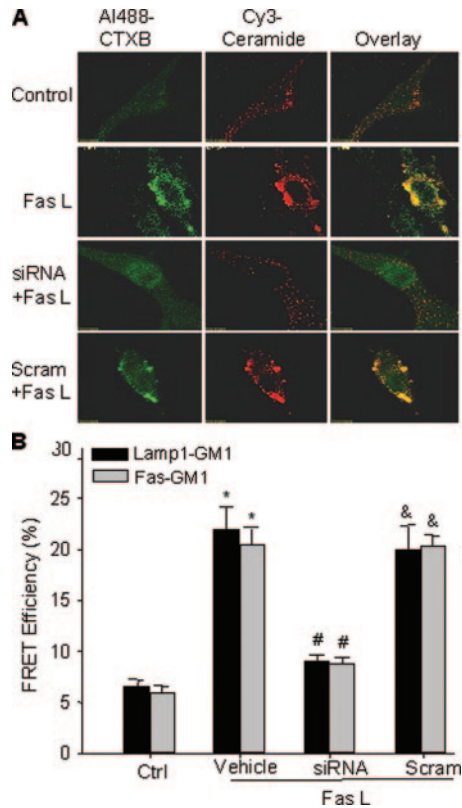
Figure 3. Representative confocal microscopic images of LR clusters and FRET efficiency between CTXB and lamp1or Fas in CAECs with sortilin gene silencing. A, Alexa488-CTX was shown as a pseudo green color on the left; Cy3-conjugated anticeramide shown as red color in the middle; and overlaid images shown on the right. Yellow spots or patches in overlaid images were defined as LRs clusters. B, FRET efficiency between CTXB and lamp1 or Fas in CAECs with sortilin gene silencing. n=6, *$P<0.05$ vs control; #$P<0.05$ vs vehicle+FasL group.

Ceramide From ASMase Pathway, but not De Novo Synthesis Pathway Contributed to the LR Platform Formation

As shown in Figure 4A, the ASMase inducer, phosphatidyl-inositol (PI, 5 μg/mL)[41] significantly increased the FRET efficiency between FITC-lamp1 and TRITC-CTXB. However, the de novo ceramide synthesis inducer, Arsenic (As$_2$O$_3$, 1 μmol/L),[42] had no significant effect on the FRET efficiency.

Caveolin-1 siRNA Failed to Block the Formation of LR Platforms

As shown in Figure 4B and 4C, after BCAECs were stimulated by FasL, some colocalization of caveolin-1 with lamp1 were observed, but not strong compared to staining with CTXB. When BCAECS were knocked down their caveolin-1 gene by a specific siRNA, the FasL-induced colocalization of lamp1 with CTXB on the membrane was still present.

FasL-Induced Lysosome Fusion Into GM1 Ganglioside-Enriched Microdomains

As shown in Figure 5A, representative images of control and FasL-stimulated BCAECs loaded with LysoTracker and Alexa488-labeled CTXB, respectively. Compared to control, FasL caused GM1 clustering on the cell membrane and colocalized with lysosomes.

FasL Caused Preloaded FM1-43 Quenched or Dequenched by BPB

As shown in Figure 5B, upper panel, without application of BPB, there are no significant changes in the FM1-43 fluorescence on FasL stimulation, because FM1-43 is not easily out of the cells. In quenching experiments, after BCAECs were loaded with 8 μmol/L FM1-43 for 2 hours, 1 mmol/L BPB were added in the extracellular solution. As shown in middle panel, FasL caused a decrease in FM1-43 fluorescence. In dequenching experiments, BCAECs were loaded simultaneously with 8 μmol/L FM1-43 and 1 mmol/L BPB for 2 hours. As shown in the lower panel, FasL caused an increase in the FM1-43 fluorescence. Supplemental Figure IV showed the colocalization of Lamp1 with AM1-43 after a prolonged incubation (2 hour).
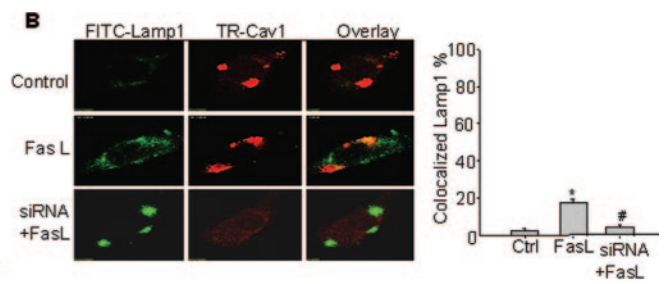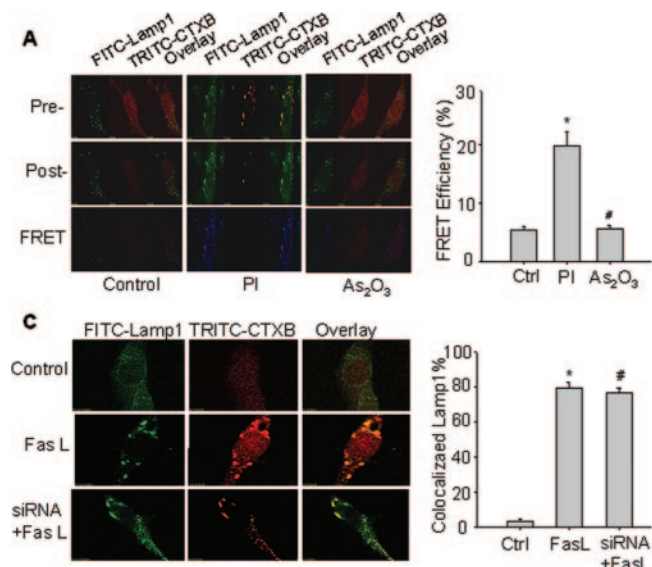
Figure 4. A, Effects of ceramide-dependent agonists, phosphatidylinositol (PI) and Arsenic (As$_2$O$_3$) on the FRET efficiency between FITC-lamp1 and TRITC-CTXB. *$P<0.05$ vs control; #$P>0.05$ vs control, n=4. B, FasL induced partial colocalization of LAMP1 with caveolin-1. *$P<0.05$ vs control; #$P<0.05$ vs FasL group, n=4. C, Caveolin-1 siRNA failed to block the FasL-induced lipid raft clustering. *$P<0.05$ vs control; #$P>0.05$ vs FasL group, n=4.
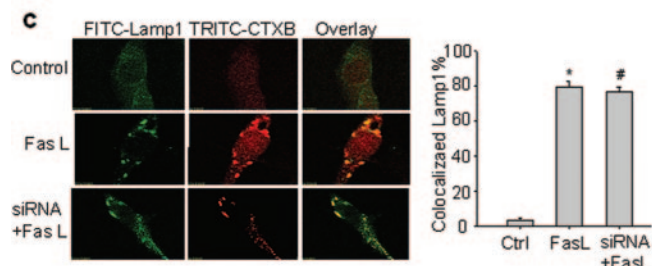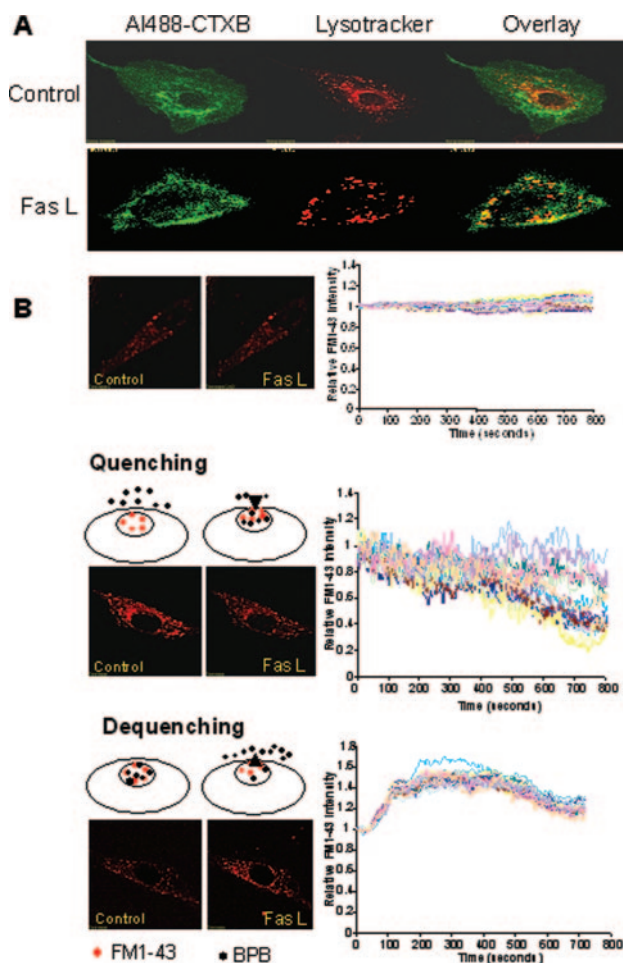
Figure 5. A, Representative images of control and FasL-stimulated (10 ng/mL for 15 minutes) BCAECs loaded with LysoTracker and Alexa488-labeled CTXB respectively B, Upper, Representative traces of FasL-induced changes of FM1-43 fluorescence, normalized by that obtained before FasL application. Middle, Representative traces of FasL-induced changes of FM1-43 fluorescence in the presence of 1 mmol/L BPB. Lower, Representative traces of FasL-induced changes of FM1-43 fluorescence in BCAECs loaded simultaneously with FM1-43 and BPB. n=4 separate experiments, respectively.

Inhibition of Lysosome Function and Knocking Down Sortilin Gene Reversed FasL-Induced Impairment of Vasodilator Response

As shown in Figure 6, compared to control, FasL significantly attenuated the BK-induced vasodilator responses in small coronary arteries. Preincubation of the arteries with Baf or GPN significantly reversed FasL-induced impairment of the vasodilator response. Pretransfection of sortilin siRNA reversed this FasL-induced action. The transfection efficiency were confirmed by FITC-labeled small RNA (supplemental Figure II).

Discussion

Because FRET can only occur between molecules in a distance within a 10-nm range,[30–33] increased FRET between lysosomal lamp1 and LRs component GM1 should indicate that some lysosomes are indeed fused into cell membrane within LR clusters. This lysosomal trafficking or fusion to the cell membrane of CAECs was dependent on the functional integrity of
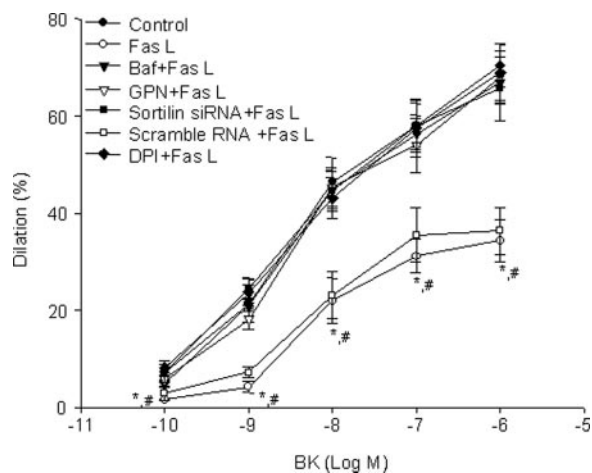

Figure 6. A, Lysosome function inhibitors and sortilin siRNA blocked the FasL-induced (10 ng/mL for 15 minutes) damage of vasodilator response. n=5, *$P<0.05$, vs control, Sortilin siRNA+FasL, DPI+FasL group; #$P>0.05$, vs Scramble+FasL group.

lysosomes in that inhibition of lysosomal function by Baf or GPN blocked FRET production between lamp1 and GM1. Besides FRET between lamp1 and GM1, we also found that between LR components GM1 and other key molecules in LR platforms, there was strong FRET production in response to Fas activation. It seems that in LR platforms or clusters may constitute a membrane complex and thus transmit and amplify signals. Although there are reports about the lysosomal fusion to the cell plasma membrane for extocytosis of different molecules,[43] to our knowledge the present results provide the first direct evidence indicating that lysosome fusion relates or contributes to the formation of LR signaling platforms, thereby participating in transmembrane signaling.

To address whether trafficking and fusion of lysosomes into the cell membrane are attributed to the formation of LR signaling platforms in CAECs, we determined the functionality of translocated or fused lysosomes in producing ceramide through a lysosome-containing enzyme ASMase in the LR platforms. Given the important role of ceramide in the formation of LR signaling platforms in various cells including CAECs,[44] demonstration of local ceramide production would indicate the formation of LR clusters, because ceramide can spontaneously aggregate to generate large macrodomains or platforms in the cell membrane.[1] By confocal microscopy, we found that FasL-induced LR platforms were indeed abundant of ceramide and that ceramide accumulation there was associated with lysosome function or fusion because inhibition of lysosomal function by Baf or GPN blocked ceramide production or accumulation in LR platforms. In additional groups of experiments, we demonstrated that local ceramide in LR platforms are colocalized with ASMase, indicating that ASMase could be the enzyme producing this sphingolipid for LR clustering. In CAECs pretreated with lysosome function inhibitors, Baf or GPN, however, there were no ceramide and ASMase clusters detected even during FasL stimulation. Taken together, all these results indicate that ASMase may be trafficking and fused into the cell membrane along with

lysosomes, where ceramide is produced and LR signaling platforms or signalosome are formed in CAECs.

To further demonstrate that ASMase accumulation in the formation of LR signaling platforms is derived from lysosomes, we examined whether targeting of this enzyme to lysosomes is involved. Previous studies have shown that ASMase targeting to lysosomes is via a sortilin-mediated process.[27] Sortilin belongs to a family of multiligand type-1 receptors with homology to the yeast receptor Vps10p, which is able to transport lysosomal proteins from the Golgi body to lysosomes.[45] In the present study, we used validated siRNA to knock down sortilin gene expression in CAECs and found that the ASMase translocation to the cell membrane and the formation of LR platforms were abolished in these CAECs with deficient gene expression of sortilin. By FRET analysis of lamp1 and LRs components, we demonstrated that silencing of sortilin gene almost completely blocked the generation of FRET between various molecular pairs in LR platforms, indicating that sortilin-mediated targeting of ASMase to lysosomes is of importance in LRs clustering. These results also further support the view that ASMase in LR platforms are derived from lysosomes. In addition, this lysosomal ASMase seems to be a driving force to activate LR clustering in CAECs, thereby leading to the formation of signaling platforms. The findings that the ASMase inducer, phosphatidylinositol (PI), but not the ceramide de novo synthesis inducer, As_2O_3, stimulated the LR platform formation indicate that only the ceramide generated through ASMase activation contributes to FasL-stimulated LR platform formation. As discussed above, lysosomal fusion process with externalization and activation of the acid sphingomyelinase occurs very rapidly after stimulation, which could be within 5 seconds.[44,46] This suggests that ASMase activation is almost simultaneously happening with lysosome fusion. If that is the case, we believe two processes are very closely coupled, where any stimuli may trigger each other almost at the same time. In our experiments, it is possible that FasL stimulation leads to lysosome trafficking and at the same time activates ASMase, resulting in lipid raft clustering. At the fusion site, activated ASMase and ceramide were brought into the membrane when fusion occurs. However, when we treated cells with ASMase activator, lysosome trafficking also happened because activation is coupled with such molecular trafficking. This supports the view that two processes are coupled well.

Next, we addressed a question whether FasL induced LR clustering is associated with caveolar behavior. We found that after stimulated by FasL, there were indeed a few colocalization of caveolin-1 with lamp1 observed, but not very strong as those with CTXB. When caveolin-1 was silenced in these cells by its specific siRNA, although the colocalization of caveolin-1 and Lamp1 was abolished, a strong CTXB-lamp1 clustering was still detected. It appears that FasL may to some extent stimulate translocation of lysosomal proteins to caveolar area, but this FasL-induced action is much weaker than that occurred in noncaveolar raft areas.

In addition, we performed more experiments to directly confirm the fusion of lysosomes to plasma membrane on FasL stimulation in BCAECs. Compared to control cells, FasL caused CTXB clustering on the cell membrane, which was very close to the lysosomes stained by LysoTracker. This further confirmed the results obtained by using lamp1 staining. We also provided direct evidence that lysosome fusion can be recorded in these cells when they were stimulated by FasL. In these experiments, FM1-43, a proved lysosome specific fluorescence dye when incubated for prolonged period (>1 hour),[35] was used to load lysosomes. This dye can be reversibly quenched by bromide phenol blue (BPB),[35] which is easier to enter or come out of the lysosomes than FM1-43. In quenching experiments, FasL was found to cause a decrease in the FM1-43 fluorescence. This was attributable to the FasL-stimulated lysosome fusion with the plasma membrane, allowing BPB to enter the lysosomes to quench FM1-43 fluorescence. In dequenching experiments, in contrast, FasL caused an increase in the FM1-43 fluorescence when lysosomes were fused to cell membrane since BPB was moved out of cells. Together, all these direct or indirect evidences strongly suggest that the fusion of lysosomes into the cell plasma membrane occurs in these BCAECs on FasL stimulation.

In our previous studies, it has been demonstrated that FasL at the dose used in the present study significantly impaired the bradykinin-induced vasodilator response.[22,25,29] The present study further found that inhibition of the lysosome function by two inhibitors or blockade of the ASMase targeting to lysosome by silencing sortilin expression with its specific siRNA significantly abolished the damaging effects of FasL. These results provide direct evidence that inhibition of lysosome function or prevention of targeting of ASMase to lysosomes may block the formation of LR platforms and thereby produce beneficial action in protecting the arterial endothelium from detrimental effects of FasL. However, it should be noted that in the present study we found that FasL-stimulated translocation of lysosomal markers is also located where the blebbing phenomenon normally took place during apoptosis (supplemental Figure III). It could be a very early functional change or signaling event during death receptors activation toward cell apoptosis. Therefore, further studies still need to be done to address some questions whether this translocation is specific for transmembrane signaling or whether this translocation is also related to apoptosis, despite that endothelial cells are relatively resistant to apoptotic stimuli.

In summary, the present study demonstrates a critical role of lysosomal trafficking and targeting of ASMase in the formation of LR signaling platforms in CAECs, which was dependent on ceramide production via lysosomal ASMase translocated into the cell membrane via a direct fusion of lysosomes to the plasma membrane. In addition, ASMase targeted to lysosomes through sortilin was the resource of this enzyme for LR signling, and failure of ASMase targeting interfered with the formation of LR signaling platforms and abolished the action of FasL as injury factor on endothelium-dependent vasodilation. It is concluded that a molecular complex in LR platforms containing both lysosomal and membrane LR molecules such as lamp1, Fas, ASMase, ceramide, and GM1 may constitute a signalosome to carry out transmembrane signal transduction during activation of Fas in CAECs.

Disclosures

None.

References

1. Bollinger CR, Teichgraber V, Gulbins E. Ceramide-enriched membrane domains. *Biochim Biophys Acta*. 2005;1746:284–294.
2. Li PL, Zhang Y, Yi F. Lipid raft redox signaling platforms in endothelial dysfunction. *Antioxid Redox Signal*. 2007;9:1457–1470.
3. Yamazaki S, Iwama A, Morita Y, Eto K, Ema H, Nakauchi H. Cytokine signaling, lipid raft clustering, and HSC hibernation. *Ann N Y Acad Sci*. 2007;1106:54–63.
4. Allen JA, Halverson-Tamboli RA, Rasenick MM. Lipid raft microdomains and neurotransmitter signalling. *Nat Rev Neurosci*. 2007;8:128–140.
5. Brown DA. Lipid rafts, detergent-resistant membranes, and raft targeting signals. *Physiology (Bethesda)*. 2006;21:430–439.
6. Cheng PC, Cherukuri A, Dykstra M, Malapati S, Sproul T, Chen MR, Pierce SK. Floating the raft hypothesis: the roles of lipid rafts in B cell antigen receptor function. *Semin Immunol*. 2001;13:107–114.
7. Cherukuri A, Dykstra M, Pierce SK. Floating the raft hypothesis: lipid rafts play a role in immune cell activation. *Immunity*. 2001;14:657–660.
8. O'Connell KM, Martens JR, Tamkun MM. Localization of ion channels to lipid Raft domains within the cardiovascular system. *Trends Cardiovasc Med*. 2004;14:37–42.
9. Romanenko VG, Fang Y, Byfield F, Travis AJ, Vandenberg CA, Rothblat GH, Levitan I. Cholesterol sensitivity and lipid raft targeting of Kir2.1 channels. *Biophys J*. 2004;87:3850–3861.
10. Harder T. Lipid raft domains and protein networks in T-cell receptor signal transduction. *Curr Opin Immunol*. 2004;16:353–359.
11. Jury EC, Kabouridis PS. T-lymphocyte signalling in systemic lupus erythematosus: a lipid raft perspective. *Lupus*. 2004;13:413–422.
12. Wollscheid B, von Haller PD, Yi E, Donohoe S, Vaughn K, Keller A, Nesvizhskii AI, Eng J, Li XJ, Goodlett DR, Aebersold R, Watts JD. Lipid raft proteins and their identification in T lymphocytes. *Subcell Biochem*. 2004;37:121–152.
13. Muller G, Schulz A, Wied S, Frick W. Regulation of lipid raft proteins by glimepiride- and insulin-induced glycosylphosphatidylinositol-specific phospholipase C in rat adipocytes. *Biochem Pharmacol*. 2005;69:761–780.
14. Muller G, Hanekop N, Wied S, Frick W. Cholesterol depletion blocks redistribution of lipid raft components and insulin-mimetic signaling by glimepiride and phosphoinositolglycans in rat adipocytes. *Mol Med*. 2002;8:120–136.
15. Muller G, Jung C, Wied S, Welte S, Frick W. Insulin-mimetic signaling by the sulfonylurea glimepiride and phosphoinositolglycans involves distinct mechanisms for redistribution of lipid raft components. *Biochemistry*. 2001;40:14603–14620.
16. Watson RT, Shigematsu S, Chiang SH, Mora S, Kanzaki M, Macara IG, Saltiel AR, Pessin JE. Lipid raft microdomain compartmentalization of TC10 is required for insulin signaling and GLUT4 translocation. *J Cell Biol*. 2001;154:829–840.
17. Hitosugi T, Sato M, Sasaki K, Umezawa Y. Lipid raft specific knockdown of SRC family kinase activity inhibits cell adhesion and cell cycle progression of breast cancer cells. *Cancer Res*. 2007;67:8139–8148.
18. Patra SK. Dissecting lipid raft facilitated cell signaling pathways in cancer. *Biochim Biophys Acta*. 2007.
19. Patra SK, Bettuzzi S. Epigenetic DNA-methylation regulation of genes coding for lipid raft-associated components: a role for raft proteins in cell transformation and cancer progression (review). *Oncol Rep*. 2007;17:1279–1290.
20. Oh HY, Lee EJ, Yoon S, Chung BH, Cho KS, Hong SJ. Cholesterol level of lipid raft microdomains regulates apoptotic cell death in prostate cancer cells through EGFR-mediated Akt and ERK signal transduction. *Prostate*. 2007;67:1061–1069.
21. Sarnataro D, Pisanti S, Santoro A, Gazzerro P, Malfitano AM, Laezza C, Bifulco M. The cannabinoid CB1 receptor antagonist rimonabant (SR141716) inhibits human breast cancer cell proliferation through a lipid raft-mediated mechanism. *Mol Pharmacol*. 2006;70:1298–1306.
22. Zhang AY, Yi F, Zhang G, Gulbins E, Li PL. Lipid raft clustering and redox signaling platform formation in coronary arterial endothelial cells. *Hypertension*. 2006;47:74–80.
23. Jin S, Zhang Y, Yi F, Li PL. Critical role of lipid raft redox signaling platforms in endostatin-induced coronary endothelial dysfunction. *Arterioscler Thromb Vasc Biol*. 2008;28:485–490.
24. Touyz RM. Lipid rafts take center stage in endothelial cell redox signaling by death receptors. *Hypertension*. 2006;47:16–18.
25. Zhang AY, Yi F, Jin S, Xia M, Chen QZ, Gulbins E, Li PL. Acid sphingomyelinase and its redox amplification in formation of lipid raft redox signaling platforms in endothelial cells. *Antioxid Redox Signal*. 2007;9:817–828.
26. Dumitru CA, Gulbins E. TRAIL activates acid sphingomyelinase via a redox mechanism and releases ceramide to trigger apoptosis. *Oncogene*. 2006;25:5612–5625.
27. Ni X, Morales CR. The lysosomal trafficking of acid sphingomyelinase is mediated by sortilin and mannose 6-phosphate receptor. *Traffic*. 2006;7:889–902.
28. Schissel SL, Keesler GA, Schuchman EH, Williams KJ, Tabas I. The cellular trafficking and zinc dependence of secretory and lysosomal sphingomyelinase, two products of the acid sphingomyelinase gene. *J Biol Chem*. 1998;273:18250–18259.
29. Jin S, Yi F, Li PL. Contribution of lysosomal vesicles to the formation of lipid raft redox signaling platforms in endothelial cells. *Antioxid Redox Signal*. 2007;9:1417–1426.
30. Kinoshita A, Fukumoto H, Shah T, Whelan CM, Irizarry MC, Hyman BT. Demonstration by FRET of BACE interaction with the amyloid precursor protein at the cell surface and in early endosomes. *J Cell Sci*. 2003;116:3339–3346.
31. Nieminen J, Kuno A, Hirabayashi J, Sato S. Visualization of galectin-3 oligomerization on the surface of neutrophils and endothelial cells using fluorescence resonance energy transfer. *J Biol Chem*. 2007;282:1374–1383.
32. Kenworthy AK, Petranova N, Edidin M. High-resolution FRET microscopy of cholera toxin B-subunit and GPI-anchored proteins in cell plasma membranes. *Mol Biol Cell*. 2000;11:1645–1655.
33. Silvius JR, Nabi IR. Fluorescence-quenching and resonance energy transfer studies of lipid microdomains in model and biological membranes. *Mol Membr Biol*. 2006;23:5–16.
34. Li N, Yi F, Sundy CM, Chen L, Hilliker ML, Donley DK, Muldoon DB, Li PL. Expression and actions of HIF prolyl-4-hydroxylase in the rat kidneys. *Am J Physiol Renal Physiol*. 2007;292:F207–F216.
35. Zhang Z, Chen G, Zhou W, Song A, Xu T, Luo Q, Wang W, Gu XS, Duan S. Regulated ATP release from astrocytes through lysosome exocytosis. *Nat Cell Biol*. 2007;9:945–953.
36. Harata NC, Choi S, Pyle JL, Aravanis AM, Tsien RW. Frequency-dependent kinetics and prevalence of kiss-and-run and reuse at hippocampal synapses studied with novel quenching methods. *Neuron*. 2006;49:243–256.
37. Kinoshita M, Hynynen K. A novel method for the intracellular delivery of siRNA using microbubble-enhanced focused ultrasound. *Biochem Biophys Res Commun*. 2005;335:393–399.
38. Taniyama Y, Tachibana K, Hiraoka K, Namba T, Yamasaki K, Hashiya N, Aoki M, Ogihara T, Yasufumi K, Morishita R. Local delivery of plasmid DNA into rat carotid artery using ultrasound. *Circulation*. 2002;105:1233–1239.
39. Li N, Chen L, Yi F, Xia M, Li PL. Salt-sensitive hypertension induced by decoy of transcription factor hypoxia-inducible factor-1alpha in the renal medulla. *Circ Res*. 2008;102:1101–1108.
40. Zhang F, Zhang G, Zhang AY, Koeberl MJ, Wallander E, Li PL. Production of NAADP and its role in Ca2+ mobilization associated with lysosomes in coronary arterial myocytes. *Am J Physiol Heart Circ Physiol*. 2006;291:H274–H282.
41. Linke T, Wilkening G, Lansmann S, Moczall H, Bartelsen O, Weisgerber J, Sandhoff K. Stimulation of acid sphingomyelinase activity by lysosomal lipids and sphingolipid activator proteins. *Biol Chem*. 2001;382:283–290.
42. Dbaibo GS, Kfoury Y, Darwiche N, Panjarian S, Kozhaya L, Nasr R, Abdallah M, Hermine O, El-Sabban M, de The H, Bazarbachi A. Arsenic trioxide induces accumulation of cytotoxic levels of ceramide in acute promyelocytic leukemia and adult T-cell leukemia/lymphoma cells through de novo ceramide synthesis and inhibition of glucosylceramide synthase activity. *Haematologica*. 2007;92:753–762.
43. Lettau M, Schmidt H, Kabelitz D, Janssen O. Secretory lysosomes and their cargo in T and NK cells. *Immunol Lett*. 2007;108:10–19.
44. Gulbins E, Li PL. Physiological and pathophysiological aspects of ceramide. *Am J Physiol Regul Integr Comp Physiol*. 2006;290:R11–R26.
45. Nielsen MS, Madsen P, Christensen EI, Nykjaer A, Gliemann J, Kasper D, Pohlmann R, Petersen CM. The sortilin cytoplasmic tail conveys Golgi-endosome transport and binds the VHS domain of the GGA2 sorting protein. *Embo J*. 2001;20:2180–2190.
46. Grassme H, Cremesti A, Kolesnick R, Gulbins E. Ceramide-mediated clustering is required for CD95-DISC formation. *Oncogene*. 2003;22:5457–5470.

Supplementary Figure Legends

SFig. 1. **A**. Intracellular lamp-1 staining.

SFig. 2. Efficiency of sortilin gene silencing in CAECs by its siRNA. A: Real time RT-PCR detection of mRNA; B: A gel document of Western blot analysis; C: Densitometric analysis of gel documents via Western blotting. Values are means ± SE; n=4, * P<0.01 vs. control; # P<0.01 vs. scrambled sRNA tranfected cells. D. Transfection of the intact endothelium of small bovine coronary arteries with scrambled small RNA labeled with fluorescein (FITC-siRNA). Control: the endothelium transfected with non-fluorescence scrambled small RNA. EC(-): the endothelium was carefully removed after FITC-siRNA transfection.

SFig. 3. A. Dynamic DIC images of a BCAEC stimulated by 10 ng/ml Fas L. Note that the location of arrowheads indicates blebs formation on the cell membrane. B. Fluorescence resonance energy transfer (FRET) between FITC-labeled lamp1 antibody and a lysosome-unrelated external protein, TRITC-conjugated anti-IgG secondary antibody in the absence (**A**) or presence (**B**) of lysosome function inhibitor, GPN. Note that only a portion of the cell was bleached and the increase in the donor fluorescence intensity only occurred in bleached area, where the intensity of donor fluorescence in non-bleached area remained almost unchanged. When lysosomal function inhibitor, 200 µM GPN was applied to pretreat the cells, this FRET can not be blocked.

SFig.4 Representative images showing the colocalization of FITC-Lamp1 and AM1-43 dye (incubation for 2 h).

Supplemental Materials About Selection of Baf and GPN

It has been reported that Baf is a macrolide antibiotic that specifically inhibits vacuolar H^+-ATPase (V-H^+-ATPase), resulting in a failure to pump protons into lysosomal lumen for acidification. Decreased acidification of lysosomal lumen has been shown to lead to loss of many lysosome functions. GPN is another mechanistically different inhibitor of lysosome function. GPN as a substrate of lysosomal cathepsin C may be hydrolysed, and its hydrolysis products could be accumulated in the vesicle, resulting in a reversible osmotic swelling and in this way interfering with lysosomal functions. It has been reported that the V-ATPase inhibitors concanamycin A and bafilomycin A lead to Golgi swelling in tobacco BY-2 cells (Protoplasma. 2004 Dec; 224(3-4):255-260). Since ASMase functions in an acidic environment, it is presumed that Baf will interfere with ASMase function. There is no report demonstrating that GPN could interact with Golgi trafficking or ASM function. This possible non-specific action on the Golgi activity is the rationale for us to use two mechanistically different tool compounds for inhibition of lysosome function.

Supplemental Protocol for Caveolin-1 Small RNA Interferrence

Based upon an established protocol of Caveolin-1 small RNA interference in bovine endothelial cells(Gonzalez E, Nagiel A, Lin AJ, Golan DE, Michel T. Small interfering RNA-mediated down-regulation of caveolin-1 differentially modulates signaling
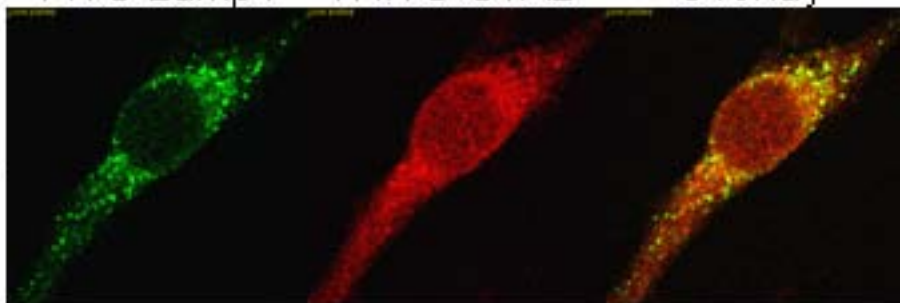
pathways in endothelial cells. J Biol Chem. 2004 Sep 24;279(39):40659-69.), we used a caveolin-1 siRNA duplex corresponding to bases 223–241 from the open reading frame of the bovine caveolin-1 mRNA: 5_-CCA GAA GGA ACA CAC AGU U-dTdT-3_, Small interfering RNA duplex oligonucleotides were purchased from QIAGEN, Inc. (Valencia, CA). transfecting BAEC at 50–70% confluence maintained in RPMI-1640/10% fetal bovine serum; transfections with siRNA (20 nM) used siLentFect^{TM}-Lipid (2:1, Bio-Rad laboratories, Hercules CA), following protocols provided by the manufacturer. Experiments were conducted 48 h after transfection. After labeling of FITC-Lamp-1, the labeling of caveolin-1 was followed. 0.3% Triton X-100 was added to each solution to permeabilize cells. Rabbit anti-caveolin-1 Antibody (1/200 dilution; BD Pharmingen) were detected with Texas red-conjugated second Antibody (1/500 dilution).
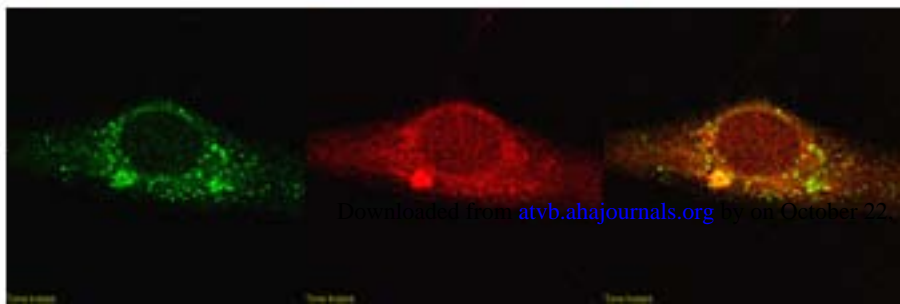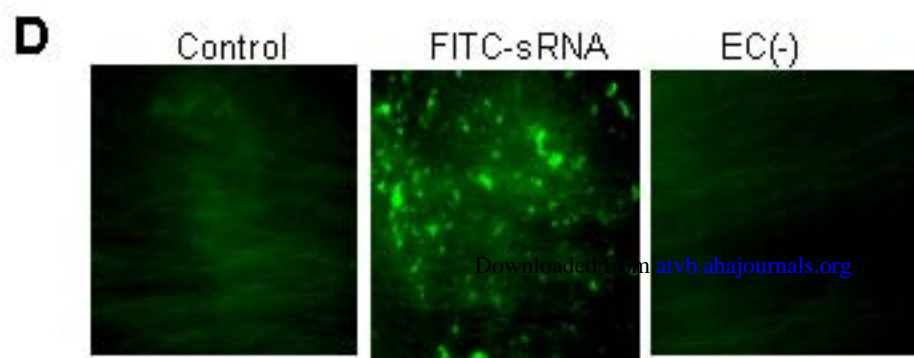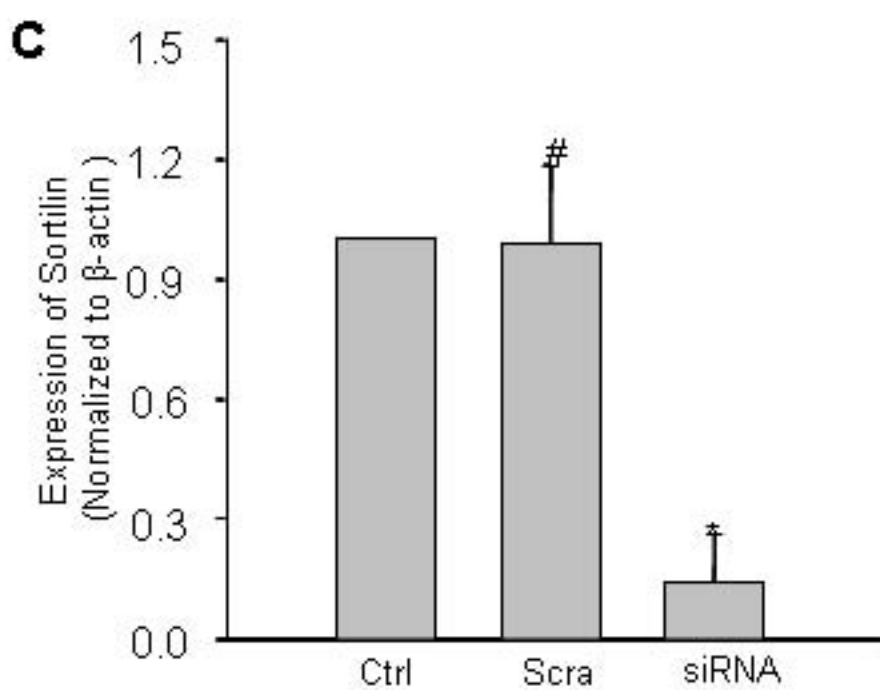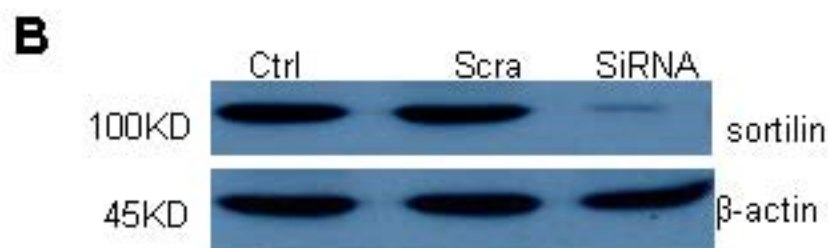
	FITC-Lamp1	TRITC-CTXB	Overlay
Control			
Fas L			

A

Relative Sortilin mRNA Level

Ctrl   Scra   siRNA

B

100KD — sortilin
45KD — β-actin

Ctrl   Scra   SiRNA

C

Expression of Sortilin
(Normalized to β-actin)

Ctrl   Scra   siRNA

D

Control   FITC-sRNA   EC(-)

A

0min   5min   10min   15min   20min

B

FITC-Lamp1   TRITC-Anti-IgG   Overlay   FITC-Lamp1   TRITC-Anti-IgG   Overlay

Pre-

Post-   bleached   bleached

FRET   bleached   bleached

GPN(-)   200 μM GPN

FITC-Lamp1   AM1-43   Overlay